

1984

## Coastal Upwelling Off The Rias Bajas, Galicia, Northwest Spain I: Hydrographic Studies

J. O. Blanton

L. P. Atkinson  
latkinso@odu.edu

F. Fernandez de Castillejo

A. Lavin Montero

Follow this and additional works at: [https://digitalcommons.odu.edu/ccpo\\_pubs](https://digitalcommons.odu.edu/ccpo_pubs)



Part of the [Oceanography Commons](#)

---

### Original Publication Citation

Blanton, J. O., Atkinson, L. P., de Castillejo, F. F., & Montero, A. L. (1984). Coastal upwelling off the Rias Bajas, Galicia, northwest Spain I: Hydrographic studies. *Rapports et procès-verbaux des réunions: The biological productivity of North Atlantic Shelf areas*, 183, 79-90.

This Article is brought to you for free and open access by the Center for Coastal Physical Oceanography at ODU Digital Commons. It has been accepted for inclusion in CCPO Publications by an authorized administrator of ODU Digital Commons. For more information, please contact [digitalcommons@odu.edu](mailto:digitalcommons@odu.edu).

# Coastal upwelling off the Rias Bajas, Galicia, Northwest Spain I: Hydrographic studies

J. O. Blanton<sup>1</sup>, L. P. Atkinson<sup>1</sup>, F. Fernandez de Castillejo<sup>2</sup>,  
and A. Lavin Montero<sup>3</sup>

Coastal upwelling occurs off the Rias Bajas of Spain between April and October. Superimposed on large-scale upwelling is a mesoscale regime of enhanced upwelling induced by topographic influences. We show that the region surrounding Cape Finisterre has intensified topographically induced upwelling.

The rias have a relatively unobstructed connection with the open ocean. Upwelling of high nitrate water on the continental shelf by Ekman transport sets up pressure gradients at the mouths of the rias that induce upwelled water to flow into the rias. Deep water in the rias responds directly to cycles of upwelling and downwelling on the continental shelf.

## Introduction

The continental shelf and rias of Galicia are among the more productive oceanic regions of the world. Located off the northwest Spanish coast (Fig. 1), the region is situated where ocean upwelling frequently supplies nutrients to shelf waters and adjacent rias. The rias themselves may also supply nutrients to the continental shelf (Tenore *et al.*, 1982), but the relative rates of export and import are not known.

This paper focuses on coastal upwelling processes and shows that water upwelled from 100–200 m fertilizes the continental shelf and rias. Upwelling is correlated with wind-driven ocean circulation. We illustrate how bathymetric influences can cause the intensity of upwelling to vary along the length of the continental shelf.

The Iberian Peninsula between latitudes 36°N and 44°N experiences upwelling-favorable winds from March through October (Wooster *et al.*, 1976). During this period, prevailing winds exert southward wind stress and Ekman transport is offshore. Coastal sea surface temperatures along the western Iberian coast are usually 2°C or more colder than surface temperatures at comparable latitudes in the middle North Atlantic Ocean. The coldest sea surface temperatures along the Iberian Peninsula are found near Lisbon where anomalies of -6°C are observed. These anomalies appear to be associated with cape-induced upwelling near Cape Roca.

<sup>1</sup>Skidaway Institute of Oceanography, P.O. Box 13687, Savannah, Georgia 31416, USA.

<sup>2</sup>Instituto Español de Oceanografía, Laboratorio Oceanográfico, Paseo de la Farola 27, Malaga, España.

<sup>3</sup>Laboratorio Oceanográfico de Santander, Promontorio de San Martín s/n, Santander, España.

Upwelling occurs when ocean currents are southward. From November to February, wind stress is generally northward, Ekman transport is onshore, and downwelling occurs. We show that deviations from this average occur, with episodes of downwelling during the upwelling season and upwelling during the downwelling season.

Fraga (1981) reviewed upwelling along the Galician coast and discussed some observations made during the summer and fall seasons. His station grid was generally

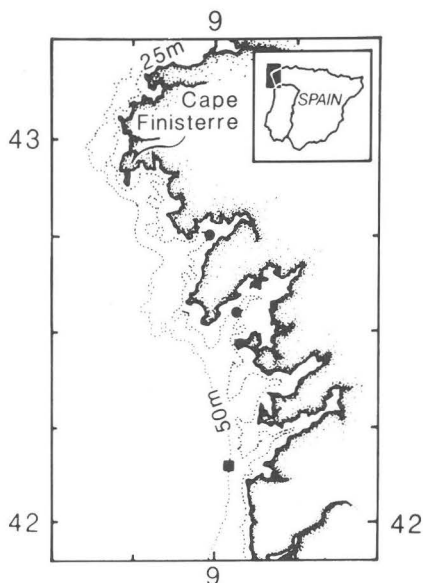


Figure 1. Location map. Solid dots mark locations of thermograph data in Ria de Muros and Ria de Arosa. Square marks location of data at mouth of Ria de Vigo.

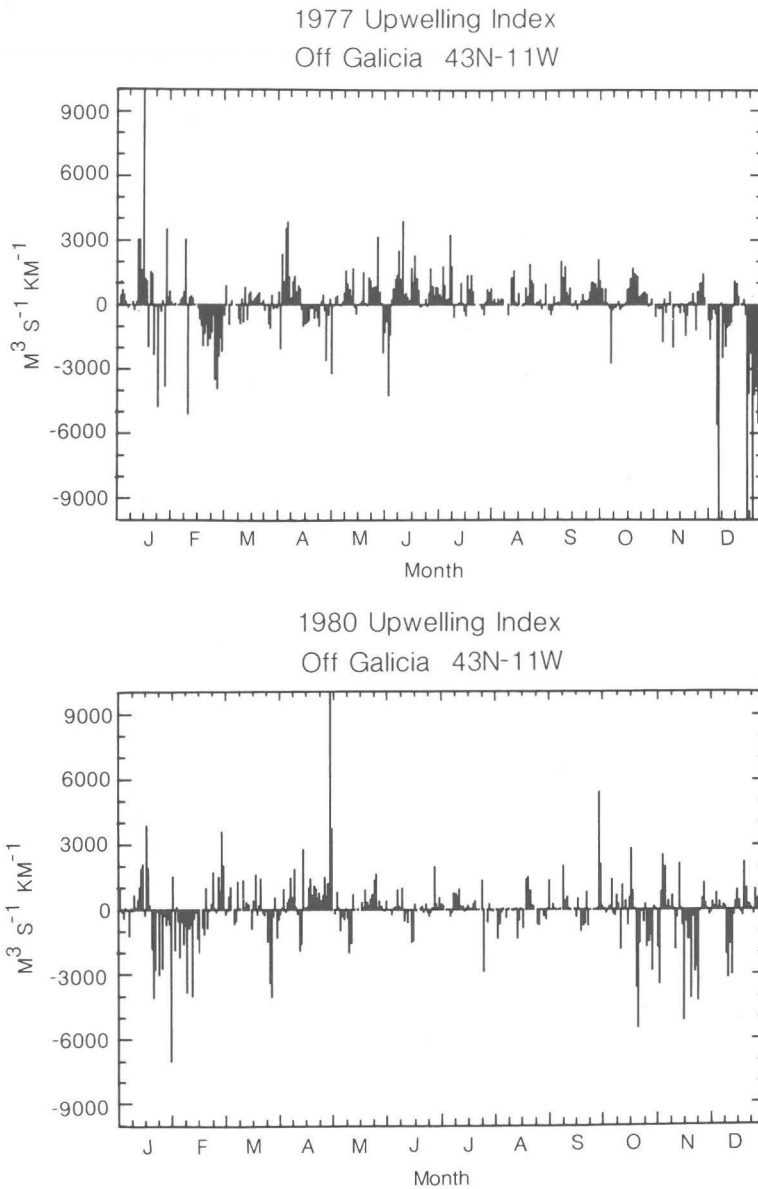


Figure 2. Upwelling indices calculated for 43°N 11°W or 150 km west of Cape Finisterre for years 1977 (top) and 1980 (bottom).

coarser than that discussed here, but his data showed the general scale of upwelling. Subsurface water along the west coast of Galicia is characteristic of North Atlantic Central Water, while that along the north coast is highly modified. Water upwelled along the north coast can be displaced by surface currents from the east. Presumably this does not occur along the west coast (Fraga, 1981).

Anomalous cold sea surface temperatures, found in the vicinity of Cape Finisterre (Margalef and Andreu, 1958) between June and September, coincide with the upwelling season defined by Wooster *et al.* (1976).

Theory predicts that upwelling is intensified downstream of topographic features such as capes, where bottom isobaths diverge. We show that upwelling on the shelf causes cold water high in nitrate to flow into the rias below the pycnocline.

In summary, the Galician coast of Spain is situated in an eastern boundary current regime that has an upwelling season lasting from April to October. Upwelling generally cools coastal sea surface temperature by 2°–5°C. There are zones of intensified upwelling near Cape Finisterre. Cool, high-nutrient upwelled water freely flows into the rias.

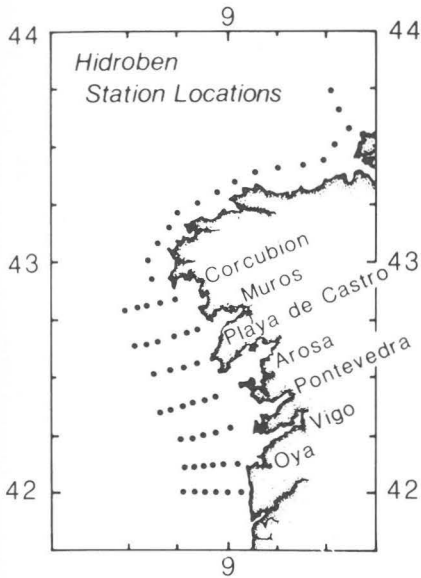


Figure 3. Station locations for April 1980 off Galicia, North-west Spain.

## Upwelling off Rias Bajas

The upwelling season can be summarized by an index representing the onshore or offshore transport of surface water. The index (Bakun, 1973) is based on Ekman transport derived from surface winds. As pointed out by Wooster *et al.* (1976), "To the extent that this transport is replaced by water from deeper layers, vertical advection is directly related to wind stress".

Ekman transport is calculated by

$$V_e = (1/f) (T \times k)$$

where  $V_e$  is the transport vector,  $T$  is wind stress at the sea surface,  $f$  is the Coriolis parameter, and  $k$  is a vertical unit vector. The components of  $V_e$  are rotated so that alongshore and offshore components conform to orientation of the local shoreline. The offshore component multiplied by 1000 m/km,  $V_{eu}$ , yields offshore volume transport per km of shoreline, a volume which presumably is replaced by vertical advection.

We calculated daily values of  $V_{eu}$  for the coast of Rias Bajas by analyzing sea surface pressure maps at 43°N 11°W (150 km west of Cape Finisterre) following the procedure of Bakun (1973). Geostrophic wind velocity was corrected for surface friction by multiplying speed by 0.7 and rotating the direction 15 degrees cyclonically (Haltiner and Martin, 1957). The results for 1977 (Fig. 2) show a predominantly positive index beginning in April and ending in mid-September agreeing well with the climatological season (Wooster *et al.*, 1976). Note, however, that while the average value of the index is positive from April to September, there are periods of negative index implying periodic reversals of

coastal currents from southward (upwelling favorable) to northward (downwelling favorable). The annual average of the index is  $V_{eu} = -220 \text{ m}^3/\text{s}/\text{km}$ , due to strong winter storms.

For 13–16 April 1981, we occupied a series of XBT and hydrographic stations between 42°N and 44°N (Fig. 3). On one portion of the cruise we ran a line of XBT stations approximately 10 km apart along the 200 m isobath. On another part of the cruise we ran a series of seven sections perpendicular to the coast from Oya (~42°N) to Corcubion (~43°N). Upwelling indices for this period indicated that downwelling-favorable winds preceded the cruise followed by a change to upwelling-favorable winds (Fig. 4).

Surface temperatures (Fig. 5) ranged from 13° to 15°C. Temperatures as high as 15.1°C occurred off the southern rias. Higher temperatures adjacent to the coast were apparently a result of downwelling just before the cruise (Fig. 4). Regions of lower temperature were found offshore of Cape Finisterre and in the extreme northern part of the study area. At the 50 m depth, horizontal temperature profiles (Fig. 5) showed upwelling of colder water with minimum temperatures of 12.8°C near the coast. A prominent minimum was found at mid-shelf off Cape Finisterre and farther north off Playa de Castro, where the coldest water at 50 m was observed.

Surface nitrate concentrations were uniformly low and typically less than 1  $\mu\text{M}$ . At 50 m, however, elevated nitrate concentrations (Fig. 6) clearly reflect coastal upwelling. Highest concentrations of 8  $\mu\text{M}$  were off Ria de Arosa and as far south as Oya (42°N). North of Ria de Arosa, inner shelf nitrate concentrations were lower except off Corcubion. Here high nitrate coincided with low temperature (Fig. 5).

Surface salinity was lowest off the rias (Fig. 7) as a result of freshwater runoff. At 50 m (Fig. 7) lower salinities near the coast reflect the salinity of upwelled North Atlantic Central Water (Fraga, 1981).

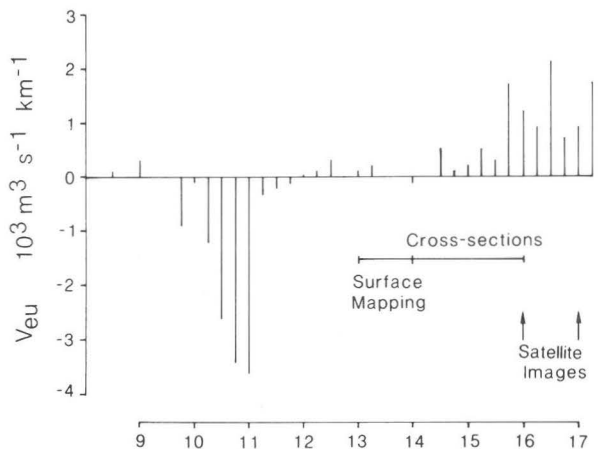


Fig. 4. Upwelling indices calculated for 43°N 11°W for the period 9–17 April 1981.

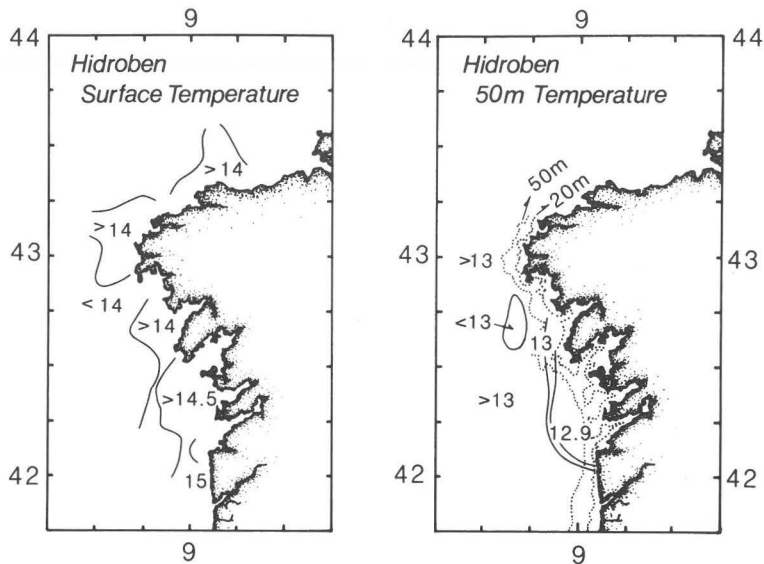


Figure 5. Distribution of temperature at surface and 50 m.

The vertical distribution of upwelling is indicated in a series of cross-shelf sections of temperature and nitrate. In the northernmost section (Fig. 8 A), no active upwelling was apparent in the temperature and nitrate

data. Downwelling was indicated at the inner shelf station (Station OC1B). Off Ria de Muros (Fig. 8 B), the same conditions prevailed, but nitrate concentrations were a little higher, especially over the outer shelf.

Off Playa de Castro (Fig. 9 A), isotherms were uplifted towards the coast and nitrate concentrations were higher than farther north. Downwelling over the inner shelf was indicated. Off Ria de Arosa (Fig. 9 B), high nitrate concentrations occurred at subsurface depths near the coast. Upwelling appeared stronger, but the nitrate distribution implies some localized downwelling at mid-shelf (Station OA4B).

Off Ria de Pontevedra (Fig. 10 A), isotherms sloped upward, then became flat on the inner shelf. Nitrate distribution suggested downwelling at station OP2B. Off Ria de Vigo (Fig. 10 B), the isotherms were practically flat and nitrate distributions again suggested downwelling (Station OV4B). Off Oya (Fig. 11) weak upwelling was indicated, with downwelling evident beyond 20 km offshore.

In summary, the cruise data indicated a general upward slope of isotherms, suggesting some upwelling although the intensity varied from section to section. Downwelling appeared active at all mid-shelf stations, apparently owing to downwelling-favorable winds that persisted during the cruise. A time history of wind stress before the cruise is at present unavailable.

We calculated the dynamic topography of the 50-dbar surface and the sea surface relative to the 100-dbar surface using the method of Helland-Hansen (1934) to extend the calculations into depths shallower than 100 m. Flow on the 50-dbar surface (Fig. 12) was southward. We speculate that general southward flow causes downwelling, which is initiated by northward wind stress. During upwelling, one normally expects poleward flow below the pycnocline (Peffley and

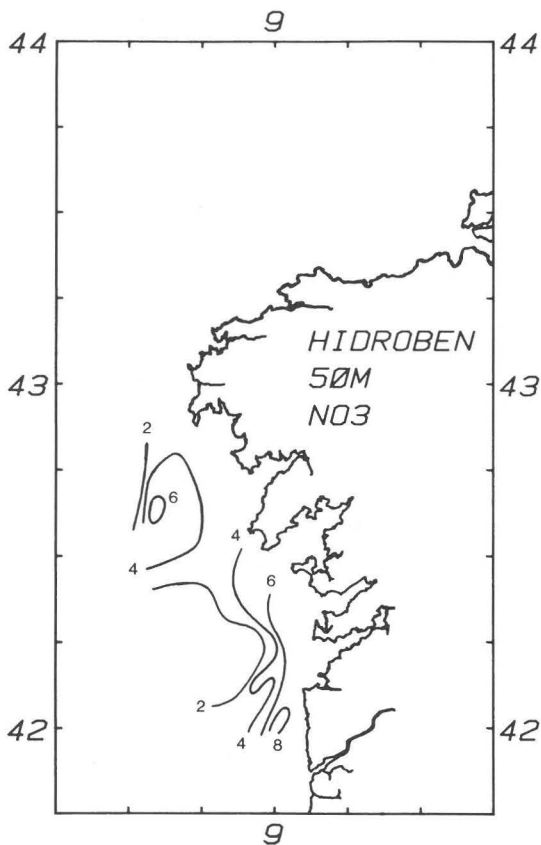


Figure 6. Distribution of nitrate at 50 m.

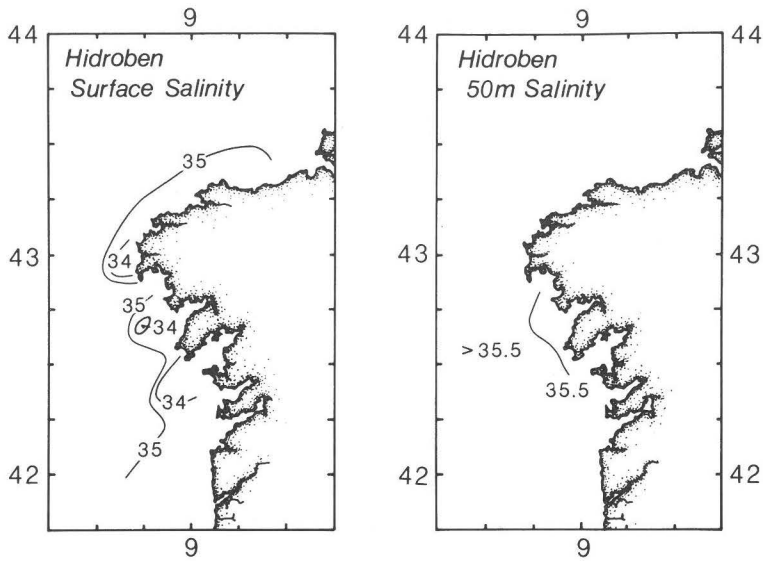


Figure 7. Distribution of salinity at surface and 50 m.

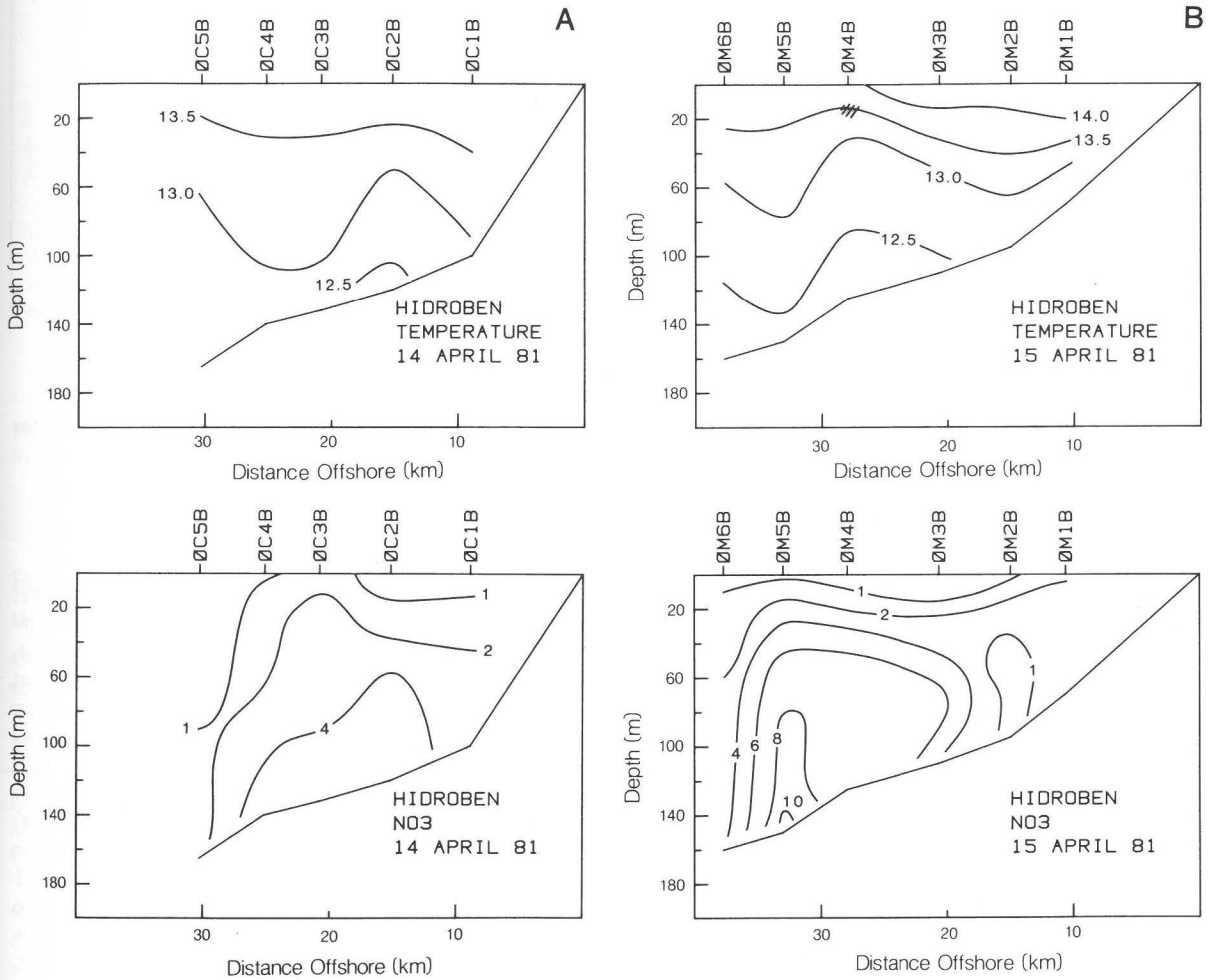


Figure 8. Cross-shelf distribution of temperature and nitrate off (A) Seno de Corcubion and (B) Ria de Muros. Refer to Figure 3 for locations. Hatched area marks temperature inversion.

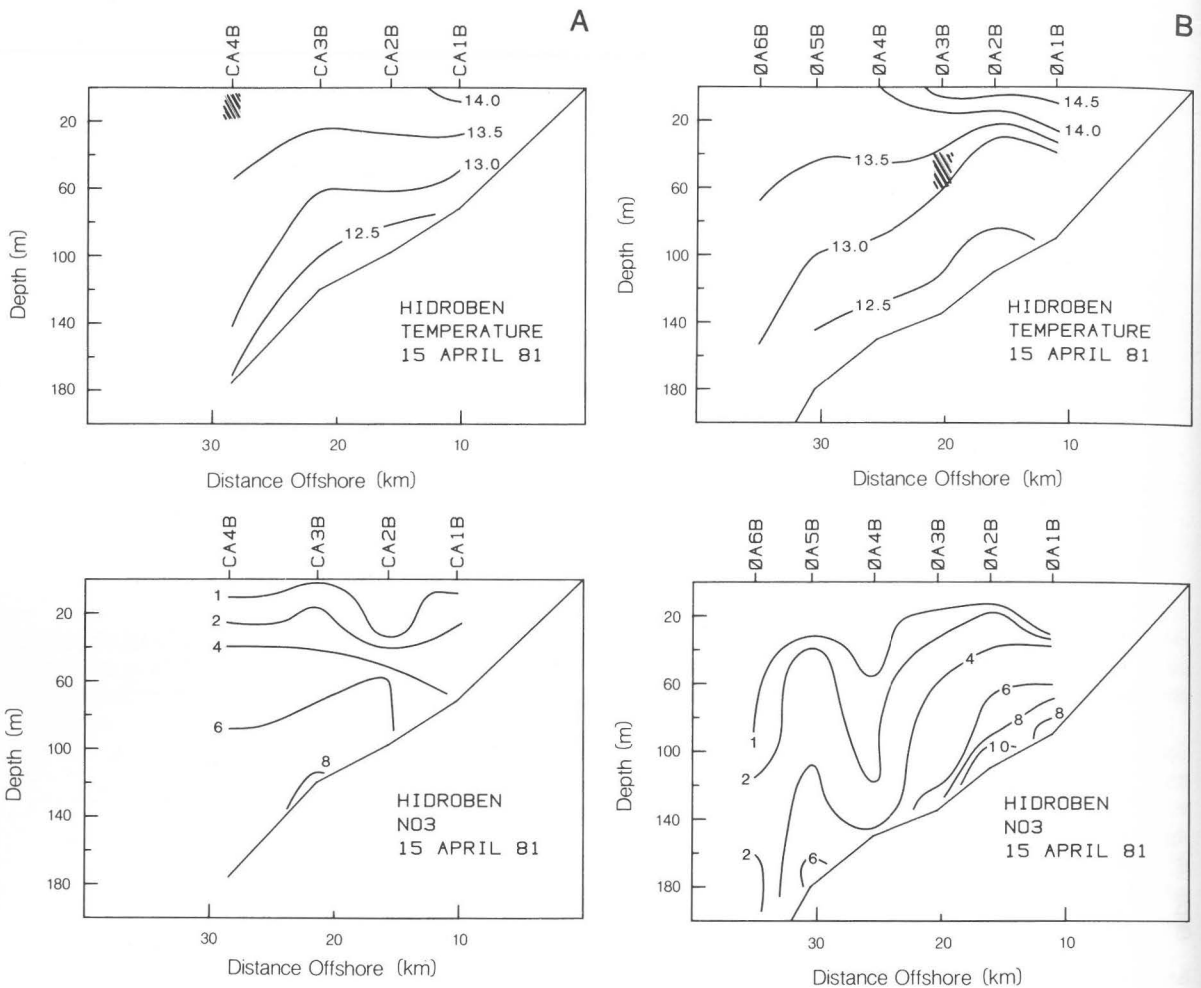


Figure 9. Cross-shelf distribution of temperature and nitrate off (A) Playa de Castro and (B) Ria de Arosa. Refer to Figure 3 for locations. Hatched areas mark temperature inversions.

O'Brien, 1976). At the northern section, a complex eddy-like structure suggested some recirculation.

Sea surface topography (Fig. 13) suggests northward flow, but the pattern is complicated by features similar in scale to those in bottom topography and shoreline configuration. Northward wind stress should cause northward water flow, but there is the suggestion of a cyclonic eddy offshore of Corcubion. The position coincides with a zone of negligible flow on the 50-dbar surface. Highest nitrate concentrations were observed at 50 m in the vicinity of the eddy. We speculate that despite a tendency for wind-induced downwelling, there was active upwelling offshore of Corcubion induced by a cyclonic eddy.

The April 1981 cruise was apparently conducted when the waters of the continental shelf were changing

from a downwelled structure to an upwelled structure. Surface temperature distribution and geostrophic currents indicated a downwelling structure (Figs. 5 and 13), but indicators of upwelling were already occurring at the 50 m level (Figs. 5, 6, and 12) off Corcubion. At the end of the cruise, upwelling-favorable winds (Fig. 4) were inducing an offshore transport at the surface. This was confirmed by two satellite images taken one day apart (Fig. 14). On April 16 warmest surface temperatures occurred adjacent to the coast, a remnant of the downwelling-favorable winds that occurred 10–11 April. The warm temperatures were separated from cooler waters offshore by a front with an average position located about 20 km offshore. One day later (Fig. 14), the front had moved an average of 13 km farther offshore as a result of offshore Ekman transport.

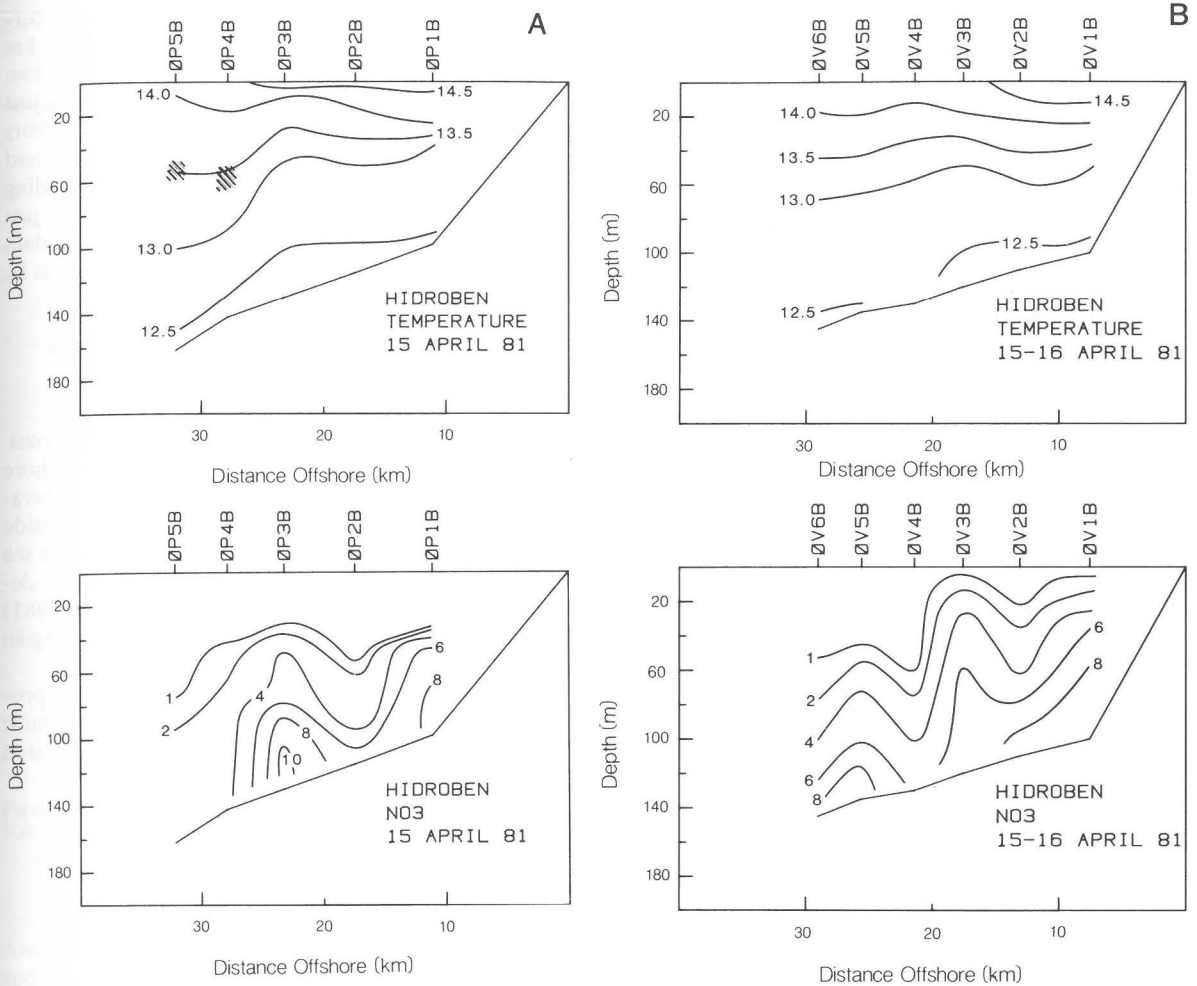


Figure 10. Cross-shelf distribution of temperature and nitrate off (A) Ria de Pontevedra and (B) Ria de Vigo. Refer to Figure 3 for locations. Hatched areas mark temperature inversions.

## Bathymetric features that enhance upwelling

Off the western coast of North America, upwelling seems to be intensified south of capes that extend out into coastal currents (Arthur, 1965). This was first noted by Japanese oceanographers in the 1930s (see Uda, 1959, for a list of references). Peffley and O'Brien (1976) demonstrated by numerical model that coastline and topographic irregularities greatly affect the longshore distribution of upwelling.

Arthur (1965) demonstrated that changes in relative vorticity along a stream line can enhance upwelling downstream of capes. The equation for conservation of vorticity is

$$f(dw/dz) = (D\eta/Dt) + \beta v$$

where  $\eta = v/R - dv/dn =$  vorticity in local coordinates of the horizontal flow ( $v$ ) along a stream line of radius of curvature  $R$ . The term  $dv/dn$  is shear normal to the stream line ( $n$ -direction);  $\beta = 2 \times 10^{-11}/\text{m/s} =$  change of planetary vorticity ( $f$ ) with latitude;  $w$  is vertical velocity along  $z$  (positive upward). The estimates below neglect  $dv/dn$  so that vorticity is calculated by  $\eta = v/R$ .

Upwelling-favorable winds along the Galician coast exert southward wind stress and induce southward coastal currents. The stream lines of water flowing around Cape Finisterre have cyclonic curvature which make  $\eta > 0$ . As water flows southward, cyclonic curvature lessens so that  $D\eta/Dt < 0$  and  $\beta v < 0$ . If the above equation is evaluated for  $w$  at 50 m, the upwelling velocity is  $2.4 \times 10^{-5}$  m/s (Table 1).

This reasoning, applied by Leming (1979) and Blan-



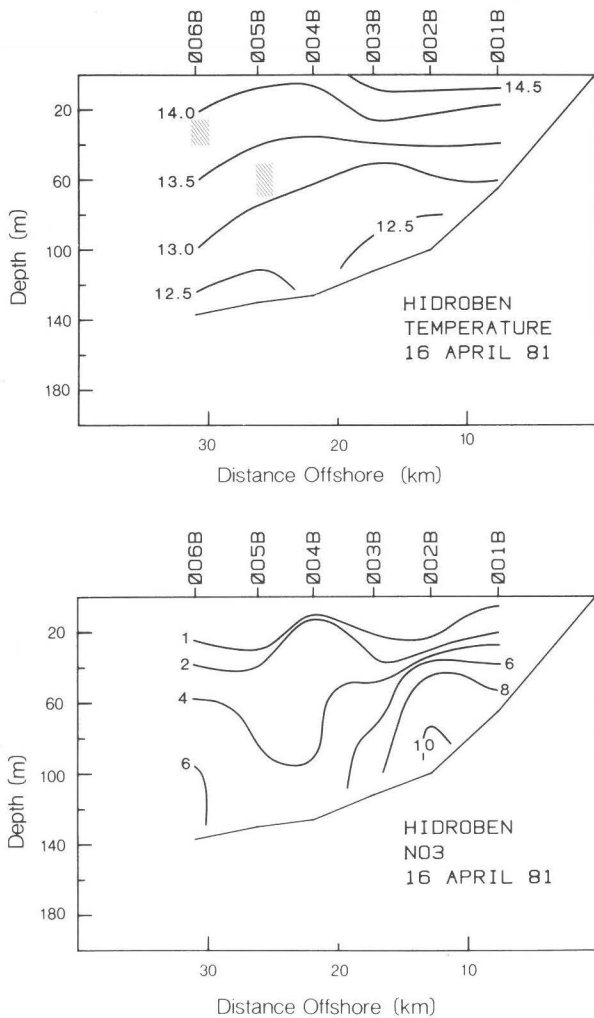


Figure 11. Cross-shelf distribution of temperature and nitrate off Oya (42°N). Refer to Figure 3 for locations. Hatched areas mark temperature inversions.

ton *et al.* (1981) to Cape Canaveral on the southeastern coast of the United States, showed that northward and southward flow induced upwelling on the north side of the Cape. The same exercise shows that upwelling is induced on the south side of Cape Finisterre under conditions of both northward and southward flows.

Table 1. Estimate of upwelling velocity in two areas of the coast of Rias Bajas. Estimates are based on the curvature of the 50 m isobath which is  $R = 50$  km in the two areas denoted in Figure 1. Flow is assumed southward at 0.3 m/s and  $w$  is estimated at a depth of 50 m. Coriolis parameter ( $f$ ) =  $10^{-4}/s$ .

$R$	= 50 km
$D\eta/Dt$	= $-5 \times 10^{-11}/s^2$
$\beta v$	= $-6 \times 10^{-12}/s^2$
$w$ (50 m)	= $+2 \times 10^{-5}$ m/s

The 50 m isobath has two regions of significant curvature (Fig. 1). Calculations done with  $R = 50$  km suggest that upwelling-favorable winds produce two zones of intensified upwelling (Table 1). The first is just downstream from Cape Finisterre. The second occurs off the mouth of Ria de Arosa. Data of Margalef and Andreu (1958) show a zone of cold water surrounding Cape Finisterre during the upwelling months, not just downstream of the Cape. We do not have adequate data to test the above theory, but our cruise data suggest its plausibility.

### Upwelling into the rias

The rias are narrow indentations into the Galician coast. On the continental shelf, wind stress sets up alongshore geostrophic currents that control the sea surface elevation at the mouths of the rias. Pressure gradients inside the rias are, in turn, controlled by fluctuations of the sea surface and pycnocline elevations. The process described here has been simulated by Klinck *et al.* (1981) wherein they describe supporting data from Norwegian fjords.

The key element of the theory is that oceanic processes at the mouth of the rias, rather than hydraulic control in the rias, control circulation. Wind-generated

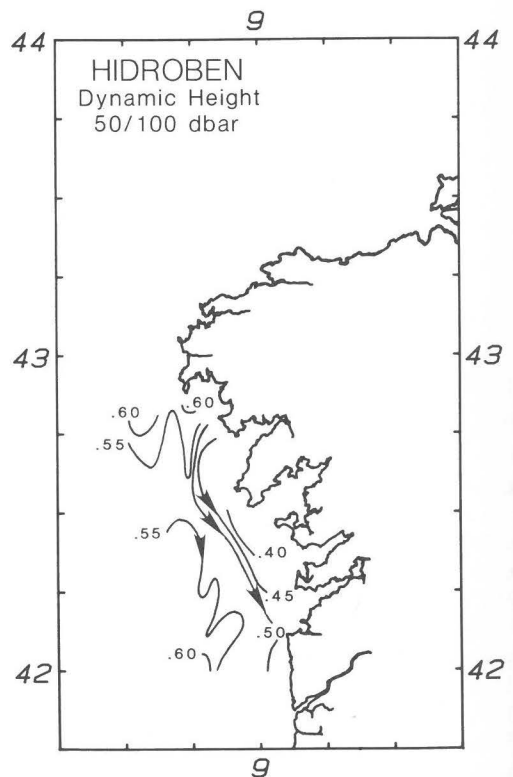


Figure 12. Dynamic height of the 50-dbar surface relative to the 100-dbar surface. Units are dynamic meters.

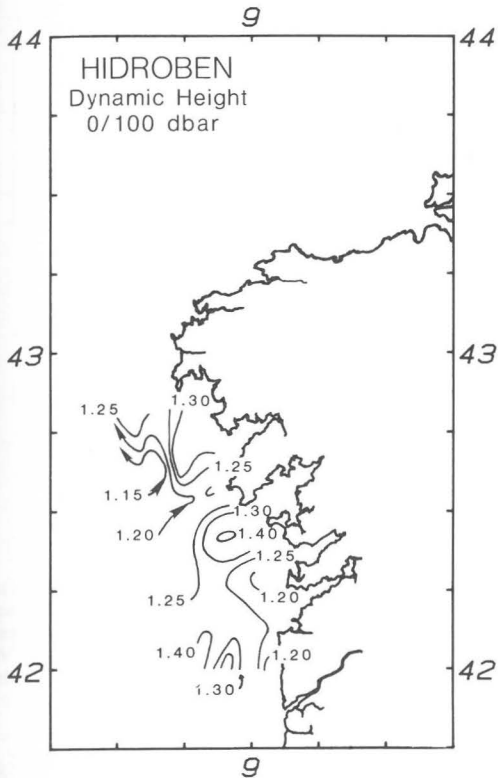


Figure 13. Dynamic height of the surface relative to the 100-dbar surface. Units are dynamic meters.

downwelling at the coast causes the sea surface to rise and the pycnocline to deepen owing to Ekman transport. Water piles up at the mouth of the ria until the pressure gradient pushes it inside. The pycnocline inside the ria deepens and water below is pushed seaward. During upwelling-favorable winds, the opposite occurs. Ekman transport lowers sea level at the mouth, setting up a seaward pressure gradient force that forces the water above the pycnocline out of the ria. The pycnocline becomes shallower and oceanic water upwelled onto the continental shelf is forced into the ria along the bottom. Theory predicts that wind stress along the axis of the ria does not produce transport that would fill or empty the ria. This is because Ekman transport to the right of the stress is along the coast, and essentially no transport is available to set up a pressure gradient at the mouth. Without this pressure gradient, water cannot be exchanged between the ocean and the ria.

Studies are in progress to test the theory. We have evidence that coastal upwelling on the shelf floods the rias with cold water high in nitrate. Fraga and Mourino (1978) published more than one year of data taken at the mouth of Ria de Vigo. We plotted these data in time series and correlated them with the upwelling indices for the same period (Fig. 15).

Note that the onset of upwelling in April is accompanied by an influx of cold water  $< 12^{\circ}\text{C}$  between depths of 30 to 50 m. Note also that the volume of cold water temporarily diminished during June when the upwelling index was lowest. The  $< 12^{\circ}\text{C}$  water was also high in nitrate with values between 5 and  $10\ \mu\text{M}$  (Fig. 3).

During 1978, we placed recording thermographs inside two rias, one at a depth of 19 m in Ria de Arosa and the other at a depth of 26 m in Ria de Muros (Fig. 1). Recorded temperatures were usually lower in Muros because the thermograph was at a greater depth. Daily averages of temperature from these two locations were correlated with daily values of upwelling indices (Fig. 16). Upwelling generally prevailed until the end of October.

Between 25 September and 4 October, upwelling indices exceeded  $50\ \text{m}^3/\text{s}/\text{km}$ . Near-bottom temperature in both rias began decreasing about one day later. In Ria de Muros, lowest temperatures occurred on 4 October, after which temperatures rose again, apparently in response to weak coastal downwelling. The next upwelling event began on 16 October. Temperatures in the rias began falling about four days later and rose again about one day after oceanic upwelling ceased. After 30 October, downwelling became more frequent as the upwelling season ended. Bottom temperatures in both rias steadily increased to the end of the record.

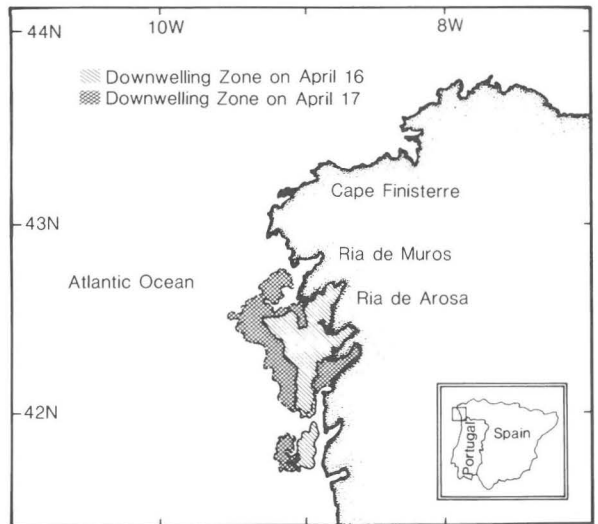


Figure 14. Demarcation of warm-water region indicated by infrared data from NOAA-6 satellite. The data came from processed images at the Image of Processing Laboratory at Rosenstiel School of Marine and Atmospheric Sciences of the University of Miami. See Figure 4 for relationship in time to the hydrographic cruise data.

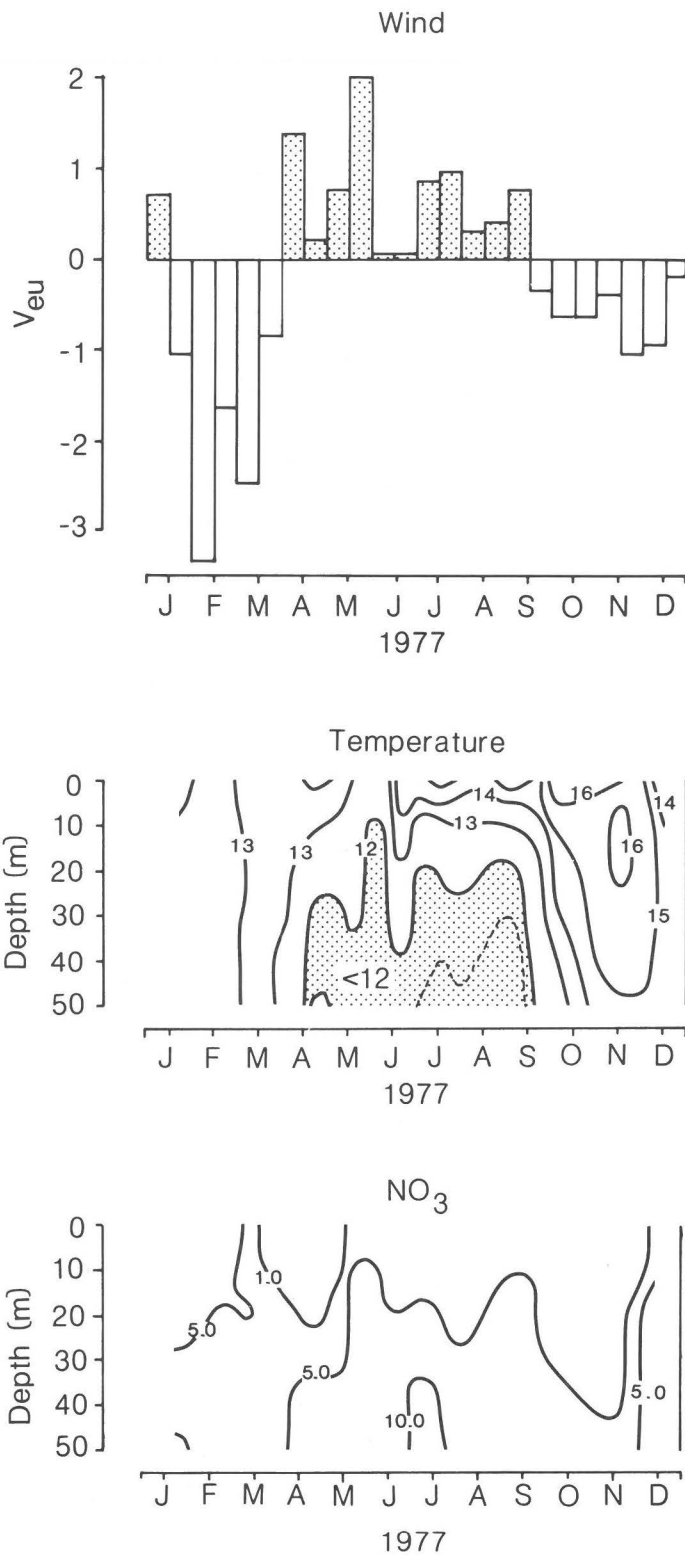


Figure 15. Correlation of upwelling indices with temperature and nitrate at the mouth of Ria de Vigo. Upwelling indices for 1977 are plotted as 15-day averages of the data in Figure 2. Data from Ria de Vigo were obtained from Fraga and Mourino (1978).

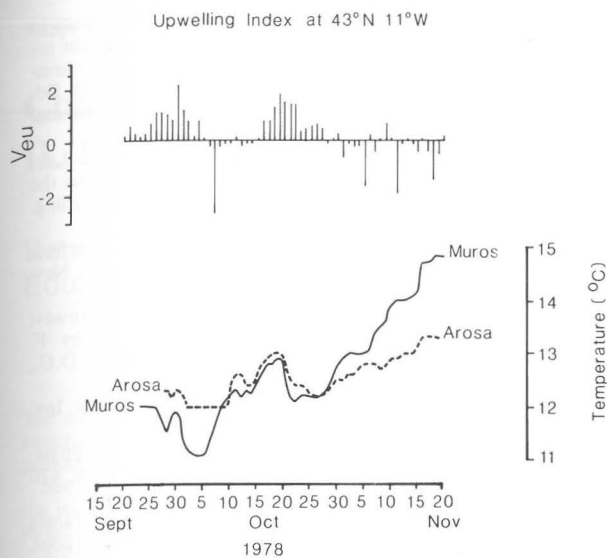


Figure 16. Correlation of upwelling indices with near-bottom temperature inside Ria de Muros and Ria de Arosa. Daily values of upwelling indices ( $10^3 \text{ m}^3/\text{s}/\text{km}$ ) calculated at  $43^\circ\text{N}$   $11^\circ\text{W}$ . Temperature data are corresponding daily averages of hourly data.

## Discussion

Ekman transport of surface water is thought to play an important role in the natural control of fish stocks near coasts (Parrish *et al.*, 1981). Coastal upwelling is a primary result of offshore Ekman transport. Here we tried to quantify that process for the Galician coast (Fig. 2). The cross-shore scale of the upwelling zone is related to the baroclinic Rossby radius of deformation,  $R_b$ , which is

$$R_b = [(\delta\rho/\rho_0)gh]^{1/2}/f$$

where  $\delta\rho$  is the density deficit of the upper layer of thickness,  $h$ ,  $\rho_0$  is the density of the lower layer,  $g$  is the acceleration of gravity, and  $f$  is the Coriolis parameter. Obviously,  $R_b$  can have a wide range of values, but typical data from Fraga (1981) and those presented here suggest that  $R_b$  can range from 5 to 15 km during observed upwelling events.

Offshore of the upwelling zone, divergence can be induced by the curl of wind stress (Fofonoff, 1963). When positive curl is found together with offshore Ekman transport, a mechanism exists which could increase the flux of nitrogen to surface layers and enhance productivity outside the coastal upwelling zone. On the other hand, if coastal upwelling occurs and the wind-stress curl is negative, convergence occurs in the Ekman layer offshore, and production is confined to the coastal upwelling zone. Parrish *et al.* (1981) argue that coastal fishery stocks may respond not only to coastal upwelling and downwelling cycles but also to seasonal cycles of

upwelling and downwelling induced by cycles of the wind-stress curl outside the upwelling zone. We hypothesize that the role coastal upwelling plays in fish production off Galicia cannot be separated from that of the seasonal cycle of wind-stress curl outside the upwelling zone.

We expect that coastal upwelling is intensified in the vicinity of Cape Finisterre. The data of Margalef and Andreu (1958) suggest that the region surrounding Cape Finisterre is anomalously cold during the upwelling season. Hydrographic data from Fraga (1981) suggest that high nitrate water is close to the surface south of Cape Finisterre. Our own hydrographic data suggest that some upwelling persists south of Cape Finisterre even during downwelling events as is predicted by the conservation of vorticity (Arthur, 1965).

Vorticity theory also predicts that upwelling is intensified in the region offshore of Ria de Arosa. The thermograph data (Fig. 16) do not support this prediction, probably because the thermographs were positioned at different depths. Thermographs should have been mounted at the same depths at the mouths of the two rias for a better test of the theory.

Upwelling indices appear to be useful indicators of coastal upwelling events. During 1977 (Fig. 2), the upwelling season was well defined and conformed to the climatological average (Wooster *et al.*, 1976). However, seasons do occur during which upwelling may be diminished (Fig. 2). During 1980, positive upwelling indices were observed beginning in April, but the index was persistently weak and variable. Studies of the variability of upwelling indices may prove valuable in predicting differences in the survival of fish larvae (Bakun and Parrish, 1980). As part of a future study, we plan to correlate deviations of upwelling indices from a 10-year average with the commercial production of mussels in Ria de Arosa.

The upwelling indices for the April 1981 cruise (Fig. 4) are useful also in predicting the offshore migration of a coastal front during upwelling. Recall that the satellite data (Fig. 14) showed that the front migrated offshore about 13 km in a 24-hour period, representing an offshore migration speed of 15 cm/s. The average value of the upwelling index for the period 16–17 April was  $1.3 \times 10^3 \text{ m}^3/\text{s}/\text{km}$  or  $1.3 \text{ m}^2/\text{s}$  (Fig. 4). If we assume the Ekman transport was confined to the upper 10 m, the depth-averaged speed is approximately 13 cm/s. We feel that it is more than fortuitous that the independent estimates of offshore speeds agree so closely. It appears that Ekman dynamics are indeed responsible for many of the changes in the coastal surface temperature field.

## Conclusions

Upwelling-favorable winds prevail off the coast of Galicia from April until October. The Rias Bajas are situated in this regime and respond to upwell-

ing-downwelling cycles in coastal upwelling. During upwelling, surface water in the rias flows seaward in response to lowered sea level. This water is replaced by cold, high nitrate oceanic water which flows into the rias along the bottom.

Intensified upwelling occurs in the vicinity of Cape Finisterre. Vorticity conservation predicts that the region lies just south of the Cape. The historical data of Margalef and Andreu (1958) and Fraga (1981) show anomalously cold coastal water north and south of Cape Finisterre, which may be a consequence of curving isobaths farther north. More interesting is the fact that the same theory predicts upwelling south of the Cape even during downwelling cycles. Our data which were obtained during a downwelling event suggest this possibility, but more study is required.

## Acknowledgements

We greatly appreciate the help of James Singer and James McClain in obtaining the recording thermograph data from Ria de Arosa and Ria de Muros. We also thank William Chandler, Lester Lamhut, and Barbara Blanton for processing the meteorological and hydrographic data. David Menzel, Ken Tenore, and Dr F. Fraga offered many helpful comments in the preparation of this paper. We are grateful to Otis Brown and Robert Evans for processing the satellite data from which Figure 14 was drawn.

## References

Arthur, R. S. 1965. On the calculation of vertical motion in eastern boundary currents from determinations of horizontal motion. *J. Geophys. Res.*, 70: 2799-2803.

Bakun, A. 1973. Coastal upwelling indices, west coast of North America, 1946-71. NOAA Tech. Rep., NMFS SSRF-671, U.S. Dept of Commerce, 103 pp.

Bakun, A., and Parrish, R. H. 1980. Environmental inputs to fishery population models for eastern boundary current regions. *In* Workshop on the effects of environmental variation on the survival of larval pelagic fishes, pp. 67-104. Ed. by G. D. Sharp. Workshop Rep. No. 28, Intergovernmental Oceanographic Commission, UNESCO, Paris.

Blanton, J. O., Atkinson, L. P., Pietrafesa, L. J., and Lee, T. N. 1981. The intrusion of Gulf Stream water across the continental shelf due to topographically induced upwelling. *Deep-Sea Res.*, 28 A: 393-405.

Fofonoff, N. P. 1963. Dynamics of ocean currents. *In* *The Sea*, pp. 232-295. Ed. by M. N. Hill, Interscience Publ., New York, N.Y., USA.

Fraga, F. 1981. Upwelling off the Galician coast, Northwest Spain. *In* Coastal upwelling, pp. 176-182. Ed. by F. Richards, American Geophysical Union, Washington, D.C., USA.

Fraga, F., and Mourino, C. 1978. Datos informativos. *Inst. Inv. Pesq.*, No. 6, 78 pp.

Haltiner, G. J., and Martin, F. L. 1957. Dynamical and physical meteorology. McGraw-Hill, New York, N.Y., USA, 470 pp.

Helland-Hansen, B. 1934. The Songenfjord section. *In* James Johnstone memorial volume, pp. 257-274. Liverpool, England.

Klinck, J. M., O'Brien, J. J., and Svendsen, H. 1981. Simple model of fjord and coastal circulation interaction. *J. phys. Oceanogr.*, 11 (12): 1612-1626.

Leming, T. D. 1979. Observations of temperature, current and wind variations off the central eastern coast of Florida. NOAA Tech. Memorandum, NMFS-SEFC-6, U.S. Dept. of Commerce, 172 pp.

Margalef, R., and Andreu, B. 1958. Componente vertical de los movimientos del agua en la Ría de Vigo y su posible relación con la entrada de sardina. *Inv. Pesq.*, 11: 105-126.

Parrish, R. H., Nelson, C. S., and Bakun, A. 1981. Transport mechanisms and reproductive success of fishes in the California Current. *Biol. Oceanogr.*, 1: 175-203.

Peffley, M. B., and O'Brien, J. J. 1976. A three-dimensional simulation of coastal upwelling off Oregon. *J. phys. Oceanogr.*, 6: 164-180.

Tenore, K. R., *et al.* 1982. Coastal upwelling in the Rias Bajas, NW Spain: Contrasting the benthic regimes of the Rias de Arosa and de Muros. *J. mar. Res.*, 40 (3): 701-772.

Uda, M. 1959. Oceanographic seminars. Manuscript Rep. Series, No. 51. Fish. Res. Bd Can, 110 pp.

Wooster, W. S., Bakun, A., and McLain, D. R. 1976. The seasonal upwelling cycle along the eastern boundary of the North Atlantic. *J. mar. Res.*, 34 (2): 131-141.